Scientific
Research
Publishing

Silicon Solar Cell Space Charge Region and Capacitance Behavior under Electric Field

Bernard Zouma[1], Fabé Idrissa Barro[2*], Prince Abdoul Aziz Honadia[1]

[1]Department of Physics, Thermal Renewable Energies Laboratory, Training and Research Unit in Exact and Applied Sciences, Joseph Ki-Zerbo University, Ouagadougou, Burkina Faso
[2]Department of Physics, Semiconductors and Solar Energy Laboratory, Faculty of Science and Technique, Cheikh Anta Diop University, Dakar, Senegal
Email: *fabe.barro@ucad.edu.sn

Abstract

This paper investigates theoretically the behavior of the space charge region of a silicon solar cell and its associated capacitance under the effect of an external electric field. The purpose of this work is to show that under illumination the solar cell's space charge region width varies with both operating point and the external induced electric field and how the solar cell capacitance varies with the space charge region width. Based on a 1D modelling of the quasi-neutral p-base, the space charge region width is determined and the associated capacitance is calculated taking into account the external electric field and the junction dynamic velocity. Based on the above calculations and simulations conducted with Mathcad, we confirmed the linear dependence of the inverse capacitance with space charge region width for thin space charge region and we exhibit an exponential dependence for large space charge region.

Keywords

Solar Cell, Electric Field, Space Charge Region, Capacitance

1. Introduction

The p-n junction remains the core of semiconductor devices; the device performance and behavior are related directly to those of this p-n junction. Among many parameters that influence the operation of the p-n junction, the injection level plays a very important role [1] [2] [3] [4]. The injection level depends on both base doping an illumination level; the base doping level controls impurities and defects level [5] with induced electric field for higher doping concentration or higher illumination level. That is, the induced electric field also plays an im-

portant role for the p-n junction.

The space charge region and the total capacitance can also characterize the p-n junction [6]. This capacitance is of major importance in switching circuits: photovoltaic power plant with DC/AC power converters or switching regulators [7] [8] where the needs are to move or remove an amount of charge as fast as possible and testing modules under flash illumination [9] [10].
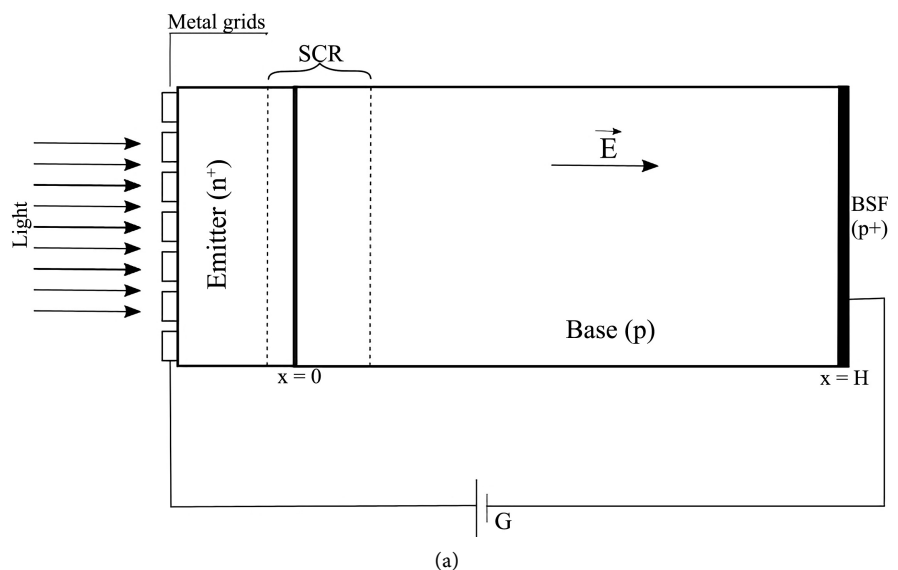
[11] and [12] analyzed the dependence of the capacitance versus space charge region width and concluded that the space charge region behaves as a plane capacitor. This means that the inverse of solar cell capacitance increases with the space charge region width. But these studies have not taken into account the effect of external electrical field.

The aim of this paper is to analyze the behavior of the space charge region and the capacitance of a forward biased silicon solar cell on the one hand, and, on the other, the relationship between the capacitance and the space charge region width for various polarization induced electric fields.

2. Mathematical Formulation

Figure 1(a) present a schematic diagram of the silicon solar cell.

When illuminated, three major phenomenon occur inside the solar cell: carrier generation, recombination and drift/diffusion. Given that the emitter thickness is typically less than 1 μm with a high doping density contrary to that of the base region (thickness up to 300 μm and doping about one hundred less than that of the emitter), the contribution of the emitter is very less than that of the base. We then neglect the emitter region and consider only the base region of the solar cell. Regarding to the space charge region width $x_E + x_B$ (**Figure 1(b)**), and considering that the emitter region is hundred times more doped than the base, x_E will then be hundred times less than x_B. Therefore, x_E is neglected and we consider that the space charge region width is x_B.
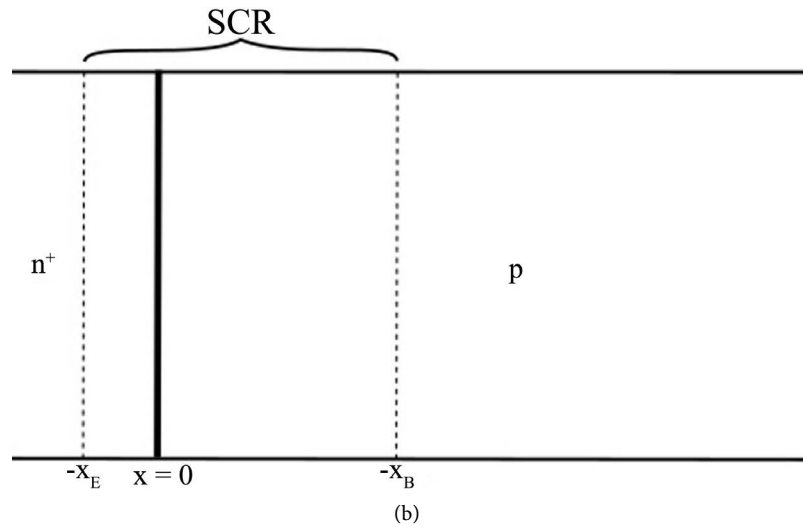

(a)

Figure 1. (a) Schematic diagram of a silicon solar cell; (b) Solar cell's space charge region.

We also assume a quasi-neutral base with low injection condition, no lateral effect and the solar cell forward biased in steady state. Then, the main transport mechanism is described by a one-dimension diffusion of minority carriers (electrons) written as [13] [14]:

$$\frac{\partial^2 \delta(x)}{\partial x^2} + \frac{\mu \cdot E}{D} \cdot \frac{\partial \delta(x)}{\partial x} - \frac{\delta(x)}{L^2} + \frac{G(x)}{D} = 0 \tag{1}$$

Let us consider $L_E = \mu \cdot E \cdot \tau$ and taking into account that $L^2 = \tau \cdot D$, Equation (1) is rewritten as:

$$\frac{\partial^2 \delta(x)}{\partial x^2} + \frac{L_E}{L} \cdot \frac{\partial \delta(x)}{\partial x} - \frac{\delta(x)}{L^2} = -\frac{G(x)}{D} \tag{2}$$

$\delta(x)$ is the excess minority carrier density, L is their diffusion length and D their diffusion coefficient.

μ is the excess minority carrier mobility and E the external induced electric field.

Carriers generation rate $G(x)$ at the depth x in the base is in the form [15] [16]:

$$G(x) = \sum_{i=1}^{3} a_i \cdot \exp(-b_i \cdot x) \tag{3}$$

a_i and b_i are tabulated values obtained from AM1.5 solar irradiance and the dependence of the absorption coefficient on the illumination wavelength [17].

The excess minority carrier density $\delta(x)$ is then given by:

$$\delta(x) = \exp(\beta \cdot x) \cdot [A \cdot \cosh(\alpha \cdot x) + B \cdot \sinh(\alpha \cdot x)] + \sum_{i=1}^{3} K_i \cdot \exp(-b_i \cdot x) \tag{4}$$

with $\alpha = \dfrac{\left(L_E^2 + 4 \cdot L^2\right)^{\frac{1}{2}}}{2 \cdot L^2}$, $\beta = \dfrac{-L_E}{2 \cdot L^2}$ and $K_i = -\dfrac{a_i \cdot L^2}{D \cdot \left[L^2 \cdot b_i^2 - L_E \cdot b_i - 1\right]}$

By help of the following boundary conditions (Equation (5) and Equation (6)),

coefficients A and B are evaluated easily:

- at the junction ($x = 0$):

$$\left.\frac{\partial\delta(x)}{\partial x}\right|_{x=0} = \frac{Sf}{D}\cdot\delta(0) \tag{5}$$

- at the backside ($x = H$):

$$\left.\frac{\partial\delta(x)}{\partial x}\right|_{x=H} = -\frac{Sb}{D}\cdot\delta(H) \tag{6}$$

H is the base thickness, Sb is the back surface velocity that traduce carrier lost at the backside of the cell; Sf is the junction dynamic velocity describing how carrier flow through the junction and is directly related to the external load conditions [18].

We now derive the capacitance C of the solar cell as follow [19] [20]:

$$C = \frac{\mathrm{d}Q}{\mathrm{d}V_{ph}} \tag{7}$$

Q is the total amount of charge across the junction and V_{ph} the photovoltage across the junction; we have $Q = q\delta(x = 0)$ with q the elementary charge.

The photovoltage result from the Boltzmann relation as:

$$V_{ph} = Vt\cdot\ln\left(\frac{Nb\cdot\delta(0)}{n_i^2} + 1\right) \tag{8}$$

Vt is the thermal voltage, n_i the intrinsic carrier concentration and Nb the base doping density.

Replacing Q by its expression and rearranging the capacitance equation, we obtain:

$$C = q\cdot\frac{\mathrm{d}\delta(x = 0)}{\mathrm{d}Sf}\cdot\frac{1}{\dfrac{\mathrm{d}V_{ph}}{\mathrm{d}Sf}} \tag{9}$$

Finally, replacing V_{ph} by the corresponding expression and doing some calculations we obtain the capacitance as [21]:

$$C = \frac{q\cdot\dfrac{n_i^2}{Nb}}{Vt} + \frac{q\delta(0)}{Vt} \tag{10}$$

3. Results and Discussion

Based on the above mathematical formulation, we performed simulation using programs written in Mathcad software with various induced fields through different forward biased voltages and various external load conditions through the dynamic junction velocity.

3.1. Relative Excess Minority Carrier Density

The relative excess minority carrier density is the ratio of the minority carrier density and the corresponding maximum value for a given operating conditions.

Figure 2 presents the relative excess minority carrier density versus the depth x in the base for various induced electric field E.

This figure shows that the excess minority carrier density increase with the depth x in the base until a maximum situated at a certain depth x_0 in the base. Above x_0, the excess minority carrier density decrease very quickly. Since illumination comes from the front side and taking into account the "Beer-Lambert" law, there are more carrier generated near the front side. Due to the presence of the junction, the photogenerated carrier in the neighborhood of the junction flow through the junction, giving rise to the observed maximum at x_0.

For increasing electric field, this maximum is left shifted leading to a space charge region width reduction; this reduction corresponds to an increase of the carrier stored in the base because there is less and less carrier flowing through the junction. This increase of the carrier stored in the base lead to an increasing capacitance. That is, the solar cell capacitance depends directly on the induced electric field.

We now present the relative excess minority carrier density versus the depth x in the base for various junction dynamic velocities (**Figure 3**).

This figure shows that the maximum of relative excess minority carrier density is also shifted according to the junction dynamic velocity but now the maximum is right shifted contrary to that obtained with the induced electric field. This behavior could be well explained by the fact that when the junction dynamic velocity Sf increase, carrier flow through the junction increase also. There are less and less free carrier in the neighborhood of the junction leading to more depleted region that is, a widening of the space charge region. The decrease in excess minority carrier density in the base and especially near the junction is
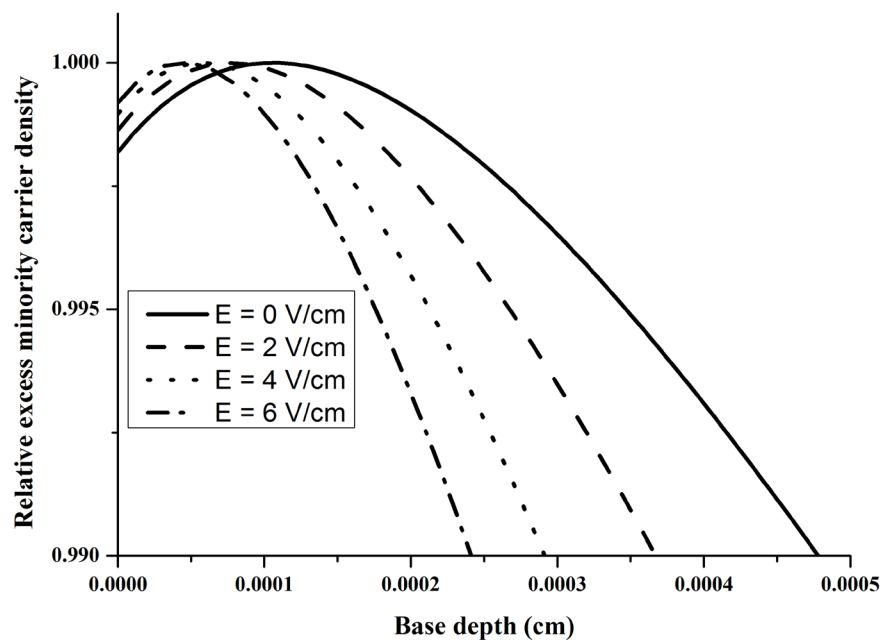

Figure 2. Relative excess minority carrier density versus base depth for various electric fields ($Sf = 10^3$ cm/s, $Sb = 10^3$ cm/s, $H = 200$ μm, $L = 100$ μm and $Nb = 10^{16}$ cm^{-3}).
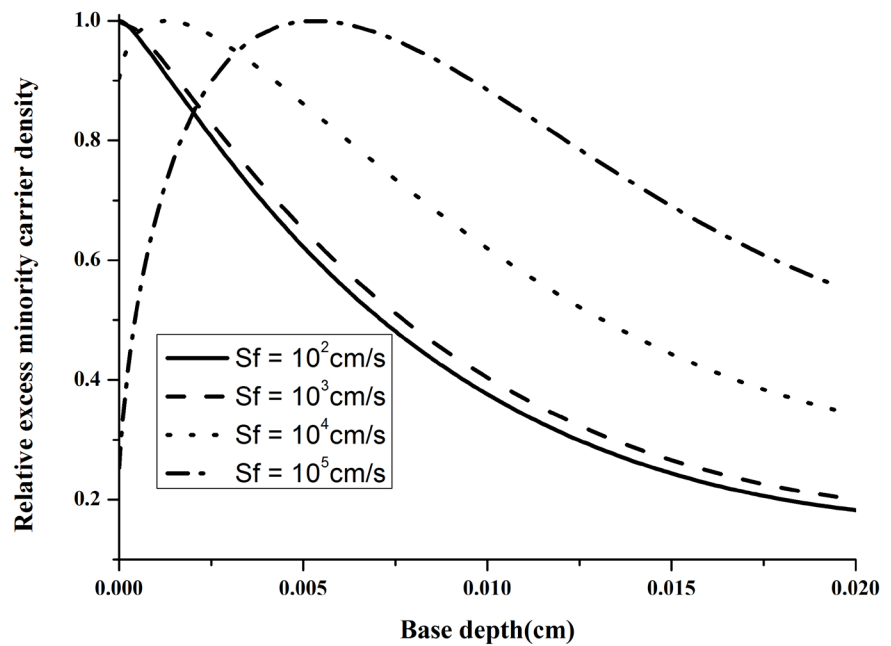
Figure 3. Relative excess minority carrier density versus base depth for various junction dynamic velocities (E = 2 V/cm, Sb = 10^3 cm/s, H= 200 μm, L = 100 μm and Nb = 10^{16} cm^{-3}).

associated to a decreasing capacitance since there is less and less free carrier stored in the base.

3.2. Space Charge Region

From the maximum of the excess minority carrier density, we have extracted the corresponding depth x_{SCR} in the base given to be the space charge region width. **Figure 4** shows how the space charge region width x_{SCR} is related to the junction dynamic velocity (semi logarithmic scale) for various induced electric fields.

As stated previously, there is a widening of the space charge region with increasing junction dynamic velocity. Near short circuit, carrier flow through the junction is very important and these carriers come mainly from the neighborhood of the junction, emptying this region and thus leading to a roll back of the maximum of the excess minority carrier density deeply in the base. That is, the more the solar cell operate near short circuit, the more the space charge region is wide.

For increasing induced electric field, more and more carriers in the bulk of the base are drifted to the neighborhood of the junction so that they can flow through the junction. Then the bulk is emptied as seen on **Figure 2** and the space charge region become thinner as observed on **Figure 4**.

3.3. Capacitance

Since charge variation in the solar cell is related to a variation of the solar cell capacitance and given that the charge variation is also related to the space charge region width, then the capacitance is directly related to the space charge region

width. To illustrate this, we have plotted in **Figure 5** the inverse capacitance versus space charge region width for various induced electric fields.

We can observe an increasing inverse capacitance with space charge region width and this increase is more marked when the space charge region is the largest for a given operating conditions. We can see in **Figure 6** that the inverse capacitance behaves linearly with respect to the space charge region width for
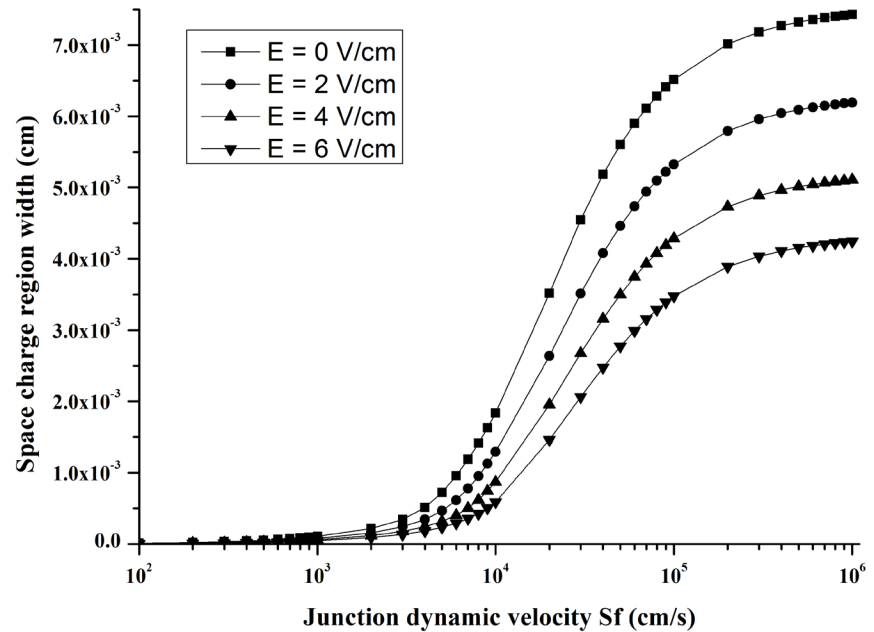

Figure 4. Space charge region width versus junction dynamic velocity for various electric fields ($Sb = 10^3$ cm/s, $H = 200$ μm, $L = 100$ μm and $Nb = 10^{16}$ cm^{-3}).
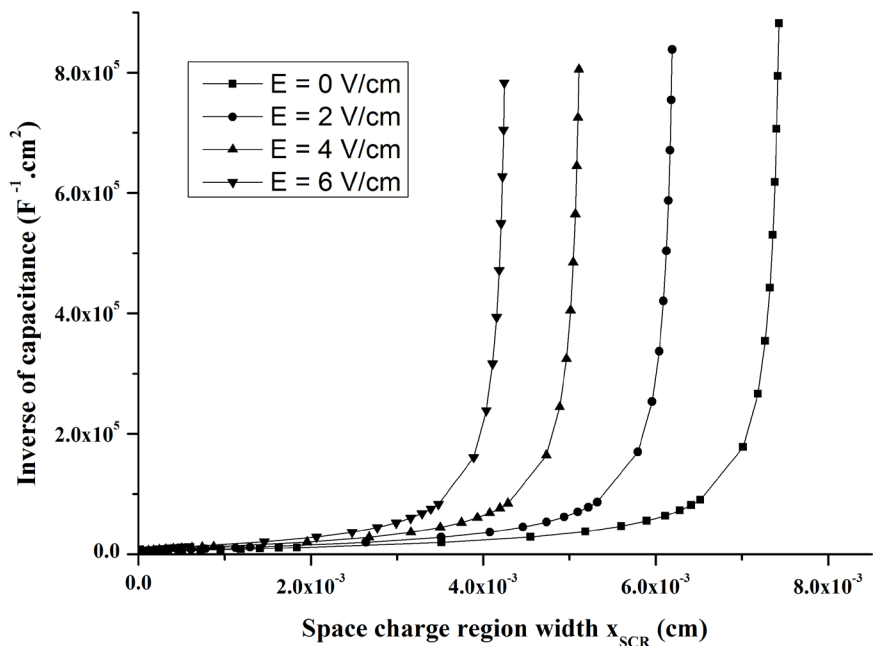

Figure 5. Inverse capacitance versus space charge region width for various electric fields ($Sf = 10^3$ cm/s, $Sb = 10^3$ cm/s, H= 200 μm, $L = 100$ μm and $Nb = 10^{16}$ cm^{-3}).

small space charge region width as previously demonstrated [11] [12]. For large space charge region width the inverse capacitance does not behaves linearly; that is, space charge region does not behaves as a plane capacitor for large values of the space charge region width.

For larger space charge region, this behavior is fitted as an exponential grow (Figure 6) in the form:

$$\frac{1}{C} = y_0 + A1 \cdot \exp\left(\frac{x - x_0}{t_1}\right) + A2 \cdot \exp\left(\frac{x - x_0}{t_2}\right) \tag{11}$$

Finally, we can write that:

$$\begin{cases} \dfrac{1}{C} = a \cdot x_{SCR} + b & \text{if } x < x_{thres} \\ \dfrac{1}{C} = y_0 + A1 \cdot \exp\left(\dfrac{x - x_0}{t_1}\right) + A2 \cdot \exp\left(\dfrac{x - x_0}{t_2}\right) & \text{if } x > x_{thres} \end{cases} \tag{12}$$

x_{thres} is a certain threshold depending on both operating conditions and base doping density; a, $A1$, $A2$, x_0, y_0, t_1 and t_2 are adjustments coefficients presented in Table 1.
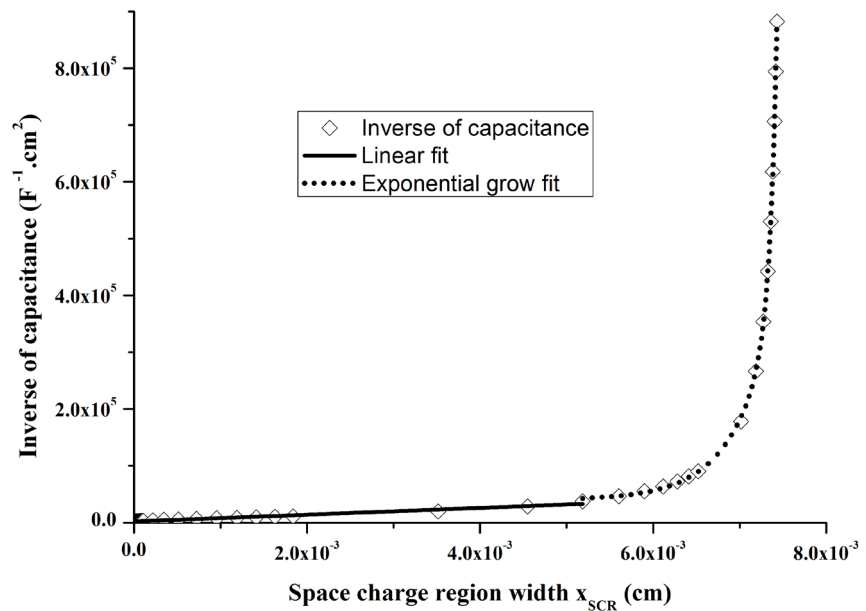

Figure 6. Theoretical fit of the inverse capacitance.

Table 1. Linear and exponential grow fit parameters.

Linear fit parameters	
Intercept (b)	2141.1187
Slope (a)	5.96156E6
Exponential grow fit parameters	
y_0	39,860.75428
x_0	0.00613

Continued

$A1$	0.01518
t_1	7.53284E−5
$A2$	21,702.42063
t_2	4.68509E−4

4. Conclusions

The behavior of the excess minority carrier density in the base of a silicon solar cell was investigated with respect to induced electric field and junction dynamic velocity. We showed that the space charge region width is directly related to both induced electric field and junction dynamic velocity. This dependence was then studied and we proved that the space charge region behaves as a plane capacitor only for thinner space charge region. For larger space charge region, based on a theoretical fit of the $1/C\text{-}x_{SCR}$ curve we pointed out a nonlinear relation (exponential growth) between the space charge region width and the inverse of the capacitance.

Future work is on the one hand experimental to validate the theoretical model used and, on the other hand, to consider 3D modeling for poly or multi-crystalline solar cells by taking into account the effects of grain boundaries.

Conflicts of Interest

The authors declare no conflicts of interest regarding the publication of this paper.

References

[1] Baskys, A., Sapurov, M. and Zubavicius, R. (2013) The New Equations of p-n Junction Carrier Injection Level. *Elektronika Ir Elektrotechnika*, **19**, 45-48. https://doi.org/10.5755/j01.eee.19.2.3467

[2] Kumar Behura, S., Mahala, P. and Ray, A. (2011) A Model on the Effect of Injection Levels over the Open-Circuit Voltage of Schottky Barrier Solar Cells. *Journal of Electron Devices*, **10**, 471-482.

[3] Yue, Y., Liou, J.J. and Ortiz-Conde, A. (1995) High-Level Injection in Quasi-Neutral Region of n/p Junction Devices: Numerical Results and Empirical Model. *Journal of Applied Physics*, **77**, 1611-1615. https://doi.org/10.1063/1.358915

[4] Meier, D.L., Hwang, J.-M. and Campbell, R.B. (1988) The Effect of Doping Density and Injection Level on Minority-Carrier Lifetime as Applied to Bifacial Dendritic Web Silicon Solar Cells. *IEEE Transactions on Electron Devices*, **ED-35**, 70-79. https://doi.org/10.1109/16.2417

[5] Geerligs, L.J. and Macdonald, D. (2004) Base Doping and Recombination Activity of Impurities in Crystalline Silicon Solar Cells. *Progress in Photovoltaics: Research and Applications*, **12**, 309-316. https://doi.org/10.1002/pip.546

[6] Neamen, D.A. (2003) Semiconductor Physics and Devices: Basic Principles. 3rd Edition, McGraw-Hill, New York.

[7] Kim, D.-K., Oh, Y.-J., Kim, S.-H., Hong, K.-J., Jung, H.-Y., Kim, H.-J. and Jeon,

M.-S. (2013) A Study of the Relationship Analysis of Power Conversion and Changed Capacitance in the Depletion Region of Silicon Solar Cell. *Transactions on Electrical and Electronic Materials*, **14**, 177. https://doi.org/10.4313/TEEM.2013.14.4.177

[8] Anil Kumar, R., Suresh, M.S. and Nagaraju, J. (2006) Effect of Solar Array Capacitance on the Performance of Switching Shunt Voltage Regulato. *IEEE Transactions on Power Electronics*, **21**, 543-548. https://doi.org/10.1109/TPEL.2005.869779

[9] Edler, A., Schlemmer, M., Ranzmeyer, J. and Harney, R. (2012) Understanding and Overcoming the Influence of Capacitance Effects on the Measurement of High Efficiency Silicon Solar Cells. *Energy Procedia*, **27**, 267-272. https://doi.org/10.1016/j.egypro.2012.07.062

[10] Roth, T., Wichmann, D., Meyer, K. and Orlob, M. (2011) In-Depth Analysis of Transient Errors of Inline IV Measurements. *Energy Procedia*, **8**, 82-87. https://doi.org/10.1016/j.egypro.2011.06.106

[11] Mbodji, S., Mbow, B., Barro, F.I and Sissoko, G. (2011) A 3D Model for Thickness and Diffusion Capacitance of Emitter-Base Junction Determination in a Bifacial Polycrystalline Solar Cell under Real Operating Condition. *Turkish Journal of Physics*, **35**, 281-291.

[12] Sissoko, G., Dieng, B., Correa, A., Adj, M. and Azilinon, D. (1998) Silicon Solar Cell Space Charge Region width Determination by a Study in Modelling. *Proceedings of the World Renewable Energy Conference*, 1852-1855.

[13] Zoungrana, M., Zerbo, I., Séré, A., Zouma, B. and Zougmore, F. (2011) 3D Study of Bifacial Silicon Solar Cell under Intense Light Concentration and under External Constant Magnetic Field. *Global Journal of Engineering Research*, **10**, 113-124.

[14] Zoungrana, M., Dieng, B., Lemrabott, O.H., Toure, F., Ould El Moujtaba, M.A., Sow, M.L. and Sissoko, G. (2012) External Electric Field Influence on Charge Carriers and Electrical Parameters of Polycrystalline Silicon Solar Cell. *Research Journal of Applied Sciences, Engineering and Technology*, **4**, 2967-2972.

[15] Furlan, J. and Amon, S. (1985) Approximation of the Carrier Generation Rate in Illuminated Silicon. *Solid-State Electronics*, **28**, 1241-1243. https://doi.org/10.1016/0038-1101(85)90048-6

[16] Mohammad, S.N. (1987) An Alternative Method for the Performance Analysis of Silicon Solar Cells. *Journal of Applied Physics*, **61**, 767-772. https://doi.org/10.1063/1.338230

[17] Rajman, K., Singh, R. and Shewchun, J. (1979) Absorption Coefficient of Silicon for Solar Cell Calculations. *Solid-State Electronics*, **22**, 793-795. https://doi.org/10.1016/0038-1101(79)90128-X

[18] Diallo, H.L., Maiga, A.S., Wereme, A. and Sissoko, G. (2008) New Approach of Both Junction and Back Surface Recombination Velocity in a 3D Modelling Study of a Polycrystalline Silicon Solar Cell. *The European Physical Journal Applied Physics*, **42**, 203-211. https://doi.org/10.1051/epjap:2008085

[19] Böer, K.W. (2010) Introduction to Space Charge Effects in Semiconductors. Springer-Verlag, Berlin. https://doi.org/10.1007/978-3-642-02236-4

[20] Hu, C.C. (2010) Modern Semiconductor Devices for Integrated Circuits. Pearson/Prentice Hall, Upper Saddle River.

[21] Barro, F.I., Sane, M. and Zouma, B. (2015) On the Capacitance of Crystalline Silicon Solar Cells in Steady State. *Turkish Journal of Physics*, **39**, 122-127. https://doi.org/10.3906/fiz-1408-3